TacFR-Gripper: A Reconfigurable Fin Ray-Based Compliant Robotic Gripper with Tactile Skin for In-Hand Manipulation

Qingzheng Cong, Wen Fan, Dandan Zhang

***Abstract*— This paper introduces the TacFR-Gripper, a novel reconfigurable soft robotic gripper inspired by the Fin Ray effect and equipped with tactile skin. The gripper incorporates a four-bar mechanism for accurate finger bending and a reconfigurable design to change the relative positions between the fingers and palm, which can enable precise and adaptable object grasping. This 5 Degree-of-Freedom (DoF) soft gripper can facilitate dexterous manipulation of objects with diverse shapes and stiffness and is beneficial to the safe and efficient grasping of delicate objects. An array of Force Sensitive Resistor (FSR) sensors is embedded within each robotic fingertip to serve as the tactile skin, enabling the robot to perceive contact information during manipulation. Moreover, we implemented a Graph Neural Network (GNN)-based tactile perception approach to enable reliable grasping without accidental slip or excessive force. To verify the effectiveness of the gripper, we provide detailed workspace analysis to evaluate the grasping performance of the gripper and conducted three experiments, including i) assess the grasp success rate across various everyday objects through different configurations, ii) verify the effectiveness of tactile skin with the GNN algorithm in grasping, iii) evaluate the gripper's in-hand manipulation capabilities for object pose control. The experimental results indicate that the TacFR-Gripper can grasp a wide range of complex-shaped objects with a high success rate and deliver dexterous in-hand manipulation. Additionally, the integration of tactile skin with the GNN algorithm enhances grasp stability by incorporating tactile feedback during manipulations. For more details of this project, please visit our website: `https://sites.google.com/view/tacfr-gripper/homepage`.**

I. Introduction

In recent years, soft and compliant robotic grippers have captured increasing attention by offering high flexibility, adaptability, and safety compared to traditional rigid grippers [1]. For example, the Fin Ray-based robotic gripper draws inspiration from the fin movements of fish to deliver a versatile and effective gripping mechanism [2]. With impressive flexibility, it can easily adapt to an object's contour, thus having a greater contact area for grasping [3]–[5]. However, most of the existing Fin Ray-based soft robotic grippers lack tactile perception, resulting in limited accuracy for grasping [6]. Moreover, they lack in-hand manipulation functions, which cannot reposition objects or adjust their poses within the robotic hand [7]–[9]. Therefore, our goal is to design and fabricate a soft Fin Ray-based reconfigurable robotic gripper integrated with tactile sensors, which can be used for dexterous in-hand manipulation tasks.

Recent advancements in soft robotic grippers, exemplified by the Belt-Augmented Compliant Hand (BACH) [10], have shed light on Fin Ray-based soft grippers for in-hand manipulation. BACH, leveraging a timing belt integrated around a compliant Fin Ray-based finger architecture, can achieve in-hand manipulation via power grasp. However, the lack of active surfaces on the palm restricts its capacity to handle objects of a wide range of sizes and shapes, especially those with irregular shapes that are too small or too large relative to the gripper. Such a timing belt for manipulation limits the weight of the handleable objects but also introduces potential robustness issues and decreased energy efficiency due to reliance on friction and sliding motions. Moreover, it does not incorporate tactile sensing for feedback control.

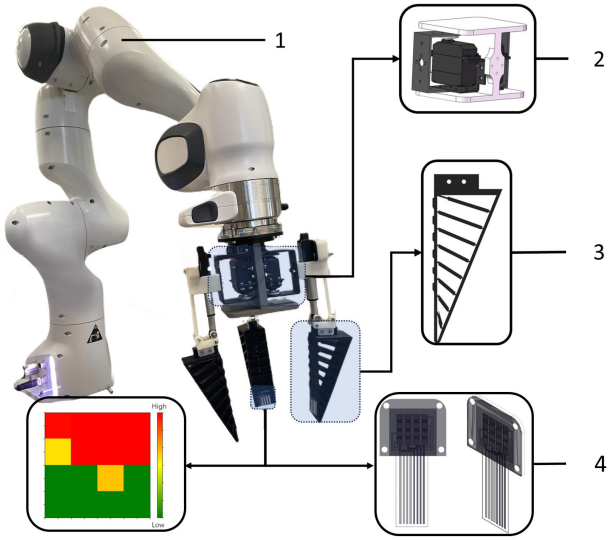

Fig. 1. Overview design of the soft gripper with tactile feedback. (1-Franka Emika Robot. 2-Reconfigurable Gripper Base driven by servo motors. 3-Fin Ray-based Finger. 4-Tactile Skin and visualization of the tactile image obtained by the embedded FSR sensor in the tactile skin.

To this end, our research aims to design a reconfigurable Fin Ray-based robotic gripper with more active joints for dexterous in-hand manipulation, while enhancing the precision of control by using a four-bar mechanism for finger bending motion control. Tactile skin, which comprises an array of sensing elements, is integrated into each fingertip to allow the gripper to perceive contact information during manipulation and adjust its grip accordingly. Also, the machine learning-based algorithm is introduced to enhance tactile data interoperability.

In summary, the **contributions** of our study are listed as follows:

- We develop a 5-DoF Fin Ray-based soft robotic gripper utilizing the 3D printing technique, which incorporates a four-bar mechanism for precise finger movement control

and features a reconfigurable mechanism in the palm. This design enables dexterous in-hand manipulation with support from extensive degrees of freedom, allowing for adaptable interaction with a variety of objects.
- We introduce a novel approach for tactile data interpretation using a Graph Neural Network (GNN), which enhances the efficiency of processing complex tactile information. This innovation advances robotic tactile perception, enabling more reliable and efficient grasping capabilities.

II. Related Work

A. Soft Robotic Gripper with Tactile Perception

Tactile sensing in soft robotic grippers can help improve object manipulation reliability by providing direct contact information, which is crucial for precise in-hand manipulation and feedback control. Sakuma et al. developed a granular-jamming-based universal soft gripper [11] with transparent filling. This gripper included an internal camera to trace markers on its surface, enabling a 3D reconstruction of the contact surface. A soft gripper named TaTa [12] incorporates RGB tricolor LEDs and employs an inbuilt camera to monitor color changes on the contact surface, significantly enhancing the resolution of the tactile image. However, integrating rigid elements such as camera modules, circuit boards, and lights into soft fingers without influencing the soft gripper's active deformation poses a challenge.

Zhao et al. introduced GelSight Svelte [13], a soft, finger-sized device that employs a camera to capture the reflection from a curved mirror, providing proprioceptive and tactile information. However, the GelSight Svelte design is limited due to its lack of compliant properties. Sandra et al. equipped a Fin Ray-based finger with the GelSight tactile sensor [14], enabling the detection of an object's pose and facilitating tactile reconstruction. This setup proved effective for reorienting a glass jar [6]. However, the delicate nature of the GelSight sensor, tightly integrated with the finger's structure, poses durability concerns. Wear and tear, such as tearing at the skin's connection to the housing or elastomer shearing from intensive manipulation or collisions, can damage the sensor. These issues potentially limit the gripper's service life and reduce its cost-effectiveness. Although tactile sensor arrays may exhibit drawbacks like relatively low resolution compared to vision-based tactile sensors [15], they have inherent advantages in terms of design flexibility and sensor adaptability. Based on soft and thin characteristics, tactile sensor arrays facilitate seamless integration into robots, and their rapid response time makes them exceptionally suited for in-hand manipulation tasks.

B. Reconfigurable Soft Gripper for In-Hand Manipulation

The reconfigurable soft gripper marks a significant advancement in the field of robotics, especially in-hand manipulation, which needs to delicately handle a wide array of objects with varying shapes and sizes. Another versatile soft robotic gripper [16] was developed with three 3D-printed soft pneumatic actuators and a reconfigurable design. It can transform among various configurations for grasping, including scoop, pinch, and claw configurations. Operating each finger independently brings its advantages in grasping diverse objects and performing intricate in-hand manipulations. However, when compared to Fin Ray-based designs, this gripper exhibits reduced strength, limiting the weight of objects it can securely grasp. Also, the inherent characteristics of the soft pneumatic actuators constrained their control precision. Furthermore, it cannot conduct dexterous in-hand manipulation due to the limited DoFs.

Batsuren et al. focused on a gripper with three pneumatic fingers [17], each containing three air chambers: two for twisting in different directions and one for grasping. This design enables the gripper to handle objects of varying shapes and sizes. This design was later improved by inserting a stiff rod that can be maneuvered inside the central hole of each finger to control the bending point [18]. This new configuration significantly enhances the dexterous grasping capabilities of the soft gripper, with a specific emphasis on in-hand manipulations. Jain et al. developed a gripper equipped with retractable fingernails and a versatile palm [19]. This innovative design enables the gripper to exert up to 1.8 N in normal grasping force and to handle objects as thin as 200 μm on flat surfaces.

III. Methodology

A. Hardware Design

1) Robot Gripper Design: Fig.2 (a) illustrates the mechanical structure of the proposed robotic gripper, while Fig.2 (b) displays the kinematic diagram of the finger and its motion range. The gripper consists of four main components: three Fin Ray-based robotic fingers, three four-bar mechanisms for controlling finger bending motion, three ST-802 mini linear actuators, and a palm equipped with two MG995 servo motors to reposition the side fingers relative to the palm. Each finger of the robotic gripper has a width of 26 mm and a height of 205 mm. The maximum distance between the two side fingers is 110 mm, which constitutes configuration 1 as shown in Fig.2 (c).

The Fin Ray-based fingers are 3D printed with Thermoplastic Polyurethane (TPU) with 95A Shore Hardness. This material can ensure a secure grip by closely conforming to various objects while retaining enough stiffness for effective force application. It significantly enhances the adaptability of robotic grippers to conform to different shapes thereby substantially increasing the contact area between the gripper and the object. Thanks to this advantage, under the same applied force, the contact pressure exerted on the object should be reduced, while the frictional force to secure the object is increased. This characteristic is particularly advantageous when handling delicate objects. Also, TPU's resilience, especially its ability to revert to its original shape post-deformation, makes it exceptionally suited for long-term, repetitive gripping tasks in robotic applications. The rest of the parts are fabricated from Polylactic acid (PLA).

The reconfiguration of the gripper is enabled by two servo motors assembled in the hollow area of the palm,

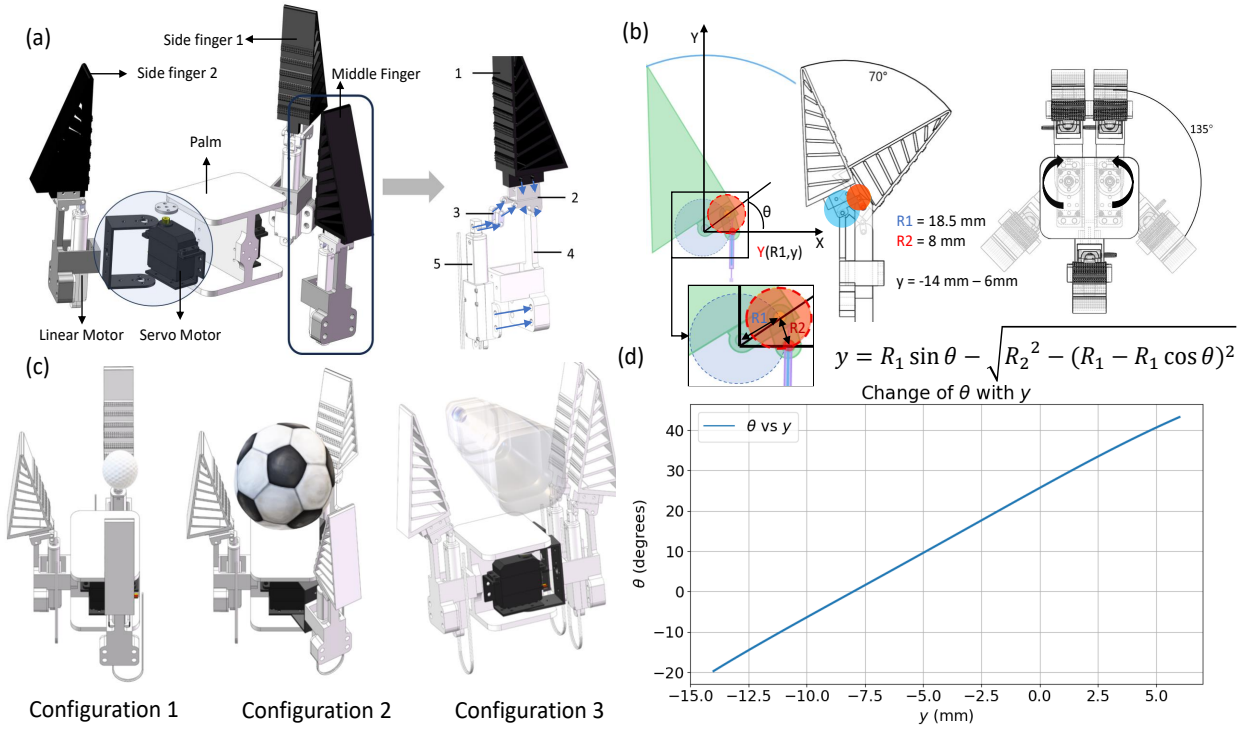

Fig. 2. Hardware overview. (a) Exploded view of the robotic gripper, 3D-printed components (1, 2, 3, 4), a four-bar mechanism, and a linear actuator (5). (b) Kinematic diagram of the finger's range of motion, with R1 and R2 denoting pivot radii, and 'y' representing the linear actuator's endpoint displacement. θ indicates the finger's bend angle. (c) Illustrative configurations of the gripper that demonstrate parallel, trigonal, and T-shaped grasps. (d) A graph of the actuator's y-displacement against finger bend angle θ based on mathematical modeling.

which grant rotational movement to the side fingers, enabling reconfigurability of the gripper. As illustrated in Fig.2 (c), the robotic gripper can adjust its gestures into three general configurations flexibly. Configuration 1 engages solely in using the side fingers to grasp targeted objects. Configuration 2 involves the collaborative effort of all three fingers, making it suitable for grasping objects with spherical shapes. Configuration 3 is used for grasping elongated objects in a horizontal position.

There is an approximately linear relationship between the coordinates of the linear actuators and the angular displacement of the finger in the four-bar linkage mechanism. This correlation is further elucidated in Fig.2 (d), where the relationship between the finger's bending angle θ, and the displacement of the linear actuator y is analyzed through mathematical modeling.

2) Sensor Array: A commercial Force Sensitive Resistor sensing array (RX-M0404S) is implemented at the fingertip of the gripper. This array functions by modifying the distribution and contact of the internal conductive filler within the composite when the external force is applied, resulting in predictable changes in resistance. Each array contains 16 sensor pixels and every pixel functions as a variable resistor, which can dynamically alter its resistance based on the applied force, thereby enabling precise distributed force measurement. As depicted in Fig.1 (4), the sensor is encased in a soft layer composed of a rubbery polymer, Agilus30, which serves to protect and balance the sensing area. This FSR array is designed to emulate human tactile perception by incorporating a dense array of mechanoreceptors.

As summarised in Table. I, more details about FSR sensor performance can be found on our project website[1].

TABLE I. Performance of the Tactile sensor

Dynamic range	2 N-25 N	**Accuracy**	6.59 %
Spatial Resolution	0.6 mm	**Temporal Resolution**	67 ms
Sensitivity	1.01	**Drift**	11 %

B. Workspace Analysis

Workspace analysis is crucial in robotics for understanding the capabilities of robotic manipulators or grippers for manipulation [20]–[22]. In this work, we iteratively generate a large number of potential finger contact locations based on the gripper's specific kinematic configurations. This approach not only highlights the accessibility of the robot's fingers but also enables a thorough exploration of the gripper's workspace. Unlike the stochastic point generation seen in the Monte Carlo method, our strategy ensures a more systematic coverage [23], [24]. Fig.3 (a) displays the potential contact points between the gripper's three fingers and the targeted object for grasping. Under the assumption that all objects are spherical, and that only three contact points (one from each finger's point cloud) will make contact with the object.

[1]https://sites.google.com/view/tacfr-gripper/sensor-calibration

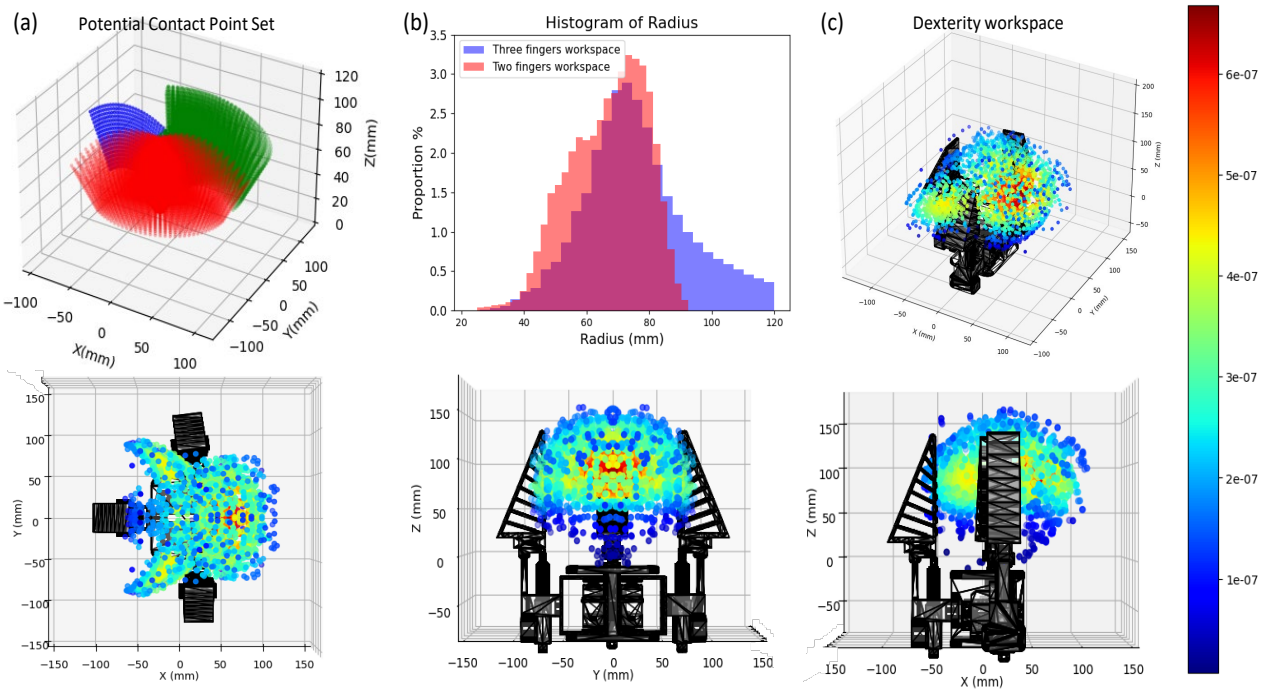

Fig. 3. (a) Visualization of the reachable workspace analysis for gripper based on points cloud-based simulation. (b) Histograms showing the distribution of circumcircle radius for Configuration 1 (red) and Configuration 2, 3 (blue), indicating the overall trend of graspable object sizes. (c) 3D view of the dexterous workspace and its cross-sectional views along the X, Y, Z axes for objects with a radius between 80 and 90 mm.

Upon establishing the coordinates of these three contact points, we can generate the direction of the force from each point, oriented perpendicularly to the finger's inner surface. By iteratively increasing the force exerted at each contact point in its specific direction, we can obtain the minimum resultant forces and torque for each point combination. An object is considered graspable if both the resultant force and torque remain beneath a predetermined threshold affected by the frictional forces and the potential deformation of the fingers. Furthermore, we calculate the circumradius of triangles defined by the points of contact on spherical objects. This circumradius directly corresponds to the sphere's radius, providing a measure of the object's size. Utilizing this radius, we construct a histogram that illustrates the gripper's dexterity with objects of specific dimensions within its total grasping range. This visual representation enables us to assess the gripper's efficacy in handling a spectrum of object sizes, highlighting its versatility. In Fig.3 (b), the red area illustrates Configuration 1, which is designed for grasping smaller objects using a pinching method. The blue area of the same figure represents Configurations 2 and 3, demonstrating the gripper's capability to handle medium and large-sized objects, specifically those with a radius ranging from 60 to 80 mm. For dexterous workspace analysis, Kernel Density Estimation (KDE) with a Gaussian kernel is utilized to create smooth, continuous density estimations [25], which illustrate the regions where the gripper is most dexterous at handling objects of various sizes.

The formula for the Gaussian kernel density estimate is:

$$f(x) = \frac{1}{n \cdot h\sqrt{2\pi}} \sum_{i=1}^{n} e^{-\frac{(x-x_i)^2}{2h^2}} \tag{1}$$

where:

- $f(x)$ is the estimated density at point x.
- n is the number of data points.
- h is the bandwidth, it is set as 0.7, which controls the width of the kernel.
- u is the standardized distance $(x - x_i)/h$, where the value represents the relative position from the center x_i, adjusted by the bandwidth h.

In Fig.3 (c), the dexterous workspace analysis and visualization of the gripper for grasping objects with varying radii (from 80 mm to 90 mm) is shown. Darker shades like blue indicate lower dexterity, while brighter regions (reds and yellows) indicate higher dexterity.

C. Tactile Perception for Grasping Stability Detection

Compliant grippers can easily adjust to different object shapes and sizes due to their flexibility, reducing the need for specific control adjustments for each geometry. However, their flexibility may affect precision in placement due to deformation. Integrating tactile sensors with grippers, such as FSR sensors, provides real-time feedback on contact information, allowing for precise control adjustments. This section compares two methods for tactile data interpretation to enhance tactile perception and demonstrates the advantages of incorporating tactile sensors.

1) Threshold-Based Method: By gradually reducing the gripping force exerted on an object, the diagonally upward support force due to gripper deformation, and friction between the contact surfaces with the object will gradually diminish until the overall upward combined force is less than the object's gravitational force. Then, the minimal force of the gripper itself required to lift without falling the object can be determined. This facilitates the calibration of the FSR sensors to fine-tune the threshold, ensuring that the force applied is just enough to maintain a secure grip without causing the object to fall. Fig.4 depicts the force curve during the grasp of an object with a suboptimal threshold setting. It clearly illustrates the initial sensor noise, followed by an oscillation phase that signifies an unstable grasp, and eventually, a stable phase where readings stabilize within the established threshold. The lowest force reading observed during the oscillation phase is indicative of the minimum force threshold, which sets the lower boundary for the force threshold. Subsequent adjustments to the threshold should therefore decrease cautiously, ensuring it remains above this critical lower limit. Through iterative testing and adjustment, the optimal force threshold can be obtained.

However, threshold-based methods require manual tuning of thresholds to adapt to different conditions, including a variety of objects, and grasping poses, lacking adaptability in real-world manipulation tasks. Therefore, a machine learning-based approach has been proposed, aiming to adapt to new operating conditions without re-tuning.

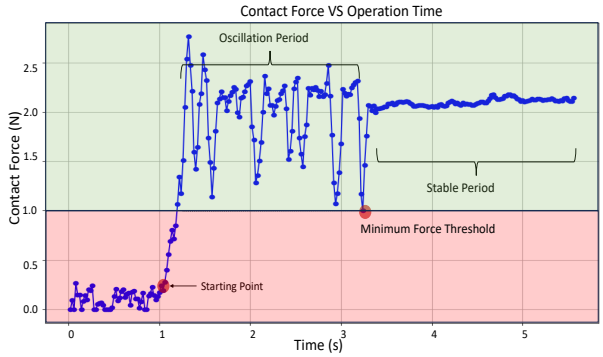

Fig. 4. Contact force recorded from a grip test: Illustration of the stable period, oscillation period during grasping, identification of the grasping starting point, and the minimum force threshold.

2) GNN-Based Method: Unlike vision sensors, such as cameras, whose output data format is standardized images, FSR sensors generate a series of discrete values, placing the challenge on applying machine learning. To address this issue, the data from FSR sensors is constructed into graph format, where each sensor unit's value is represented as a node, and connected to the adjacent neighbors through the edges. A 4x4 sensor array is used as an example, while 84 edges are formed within each sensor array. We use a Graph Convolutional Network (GCN) [26] in this paper, which is a popular version of GNN and has shown great performance on several tasks. This approach learns features by inspecting neighboring nodes and aggregating node features through

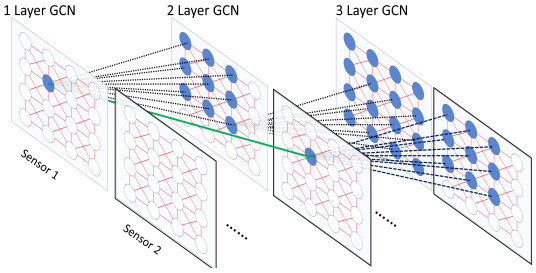

Fig. 5. GCN Architectures with 3 layers for sensor data integration. Blue dots represent sensor nodes, connected within sensor arrays by red lines for local feature extraction, and across arrays by green lines for data integration.

the convolutional layer [27]. The inner connections within each layer are represented by dotted lines, as shown in Fig.5. Considering the cooperation work of the three fingers in the gripping manipulation, each node is additionally connected to its corresponding nodes in the other two sensor arrays, effectively integrating data across three sensors and adding 32 edges per sensor. These inter-array connections are highlighted with green lines. In total, each graph data comprises 348 edges, enabling the GCN to aggregate features from multiple layers. This process facilitates the analysis and extraction of intricate spatial relationships among the sensor arrays. By aggregating information from each node's immediate neighborhood in the first layer, and incrementally broadening this scope in subsequent layers, the GCN significantly enhances its capability to identify complex patterns across the three distinct sensor data sets. Here to train the GCN model, we collected a dataset from experiments using a threshold-based method, categorizing samples under the minimum force threshold (red part) as 0 (Non-Graspable) and those above (green part) as 1 (Graspable), as depicted in Fig.4. The dataset encompasses 2100 training and 700 test samples. In this study, a three-layer GCN model trained on this dataset could achieve a high test accuracy of 96.2%.

IV. Experiments

A. Gripping Capability Evaluation

The first experiment aims to assess the gripping capability. In this experiment, the gripper engages with different objects and repeatedly grasps them ten times to evaluate the success rate across three different configurations. The properties of the objects used in the gripping experiments are summarized in Table.II, listing from lightest to heaviest objects. The term Dimensions (d × h) refers to the diameter multiplied by the height.

The results of the experiment are shown in Fig. 6, where the different colors of bars represent different configurations. As indicated by the prior analysis of the workspace, the gripper encounters difficulties with objects that are either too small (less than 10 mm in radius) or too large (exceeding 125 mm in radius). However, thanks to the gripper's reconfigurable capability, allowing various configurations to leverage their unique strengths. The optimal success rate is 97.5%,

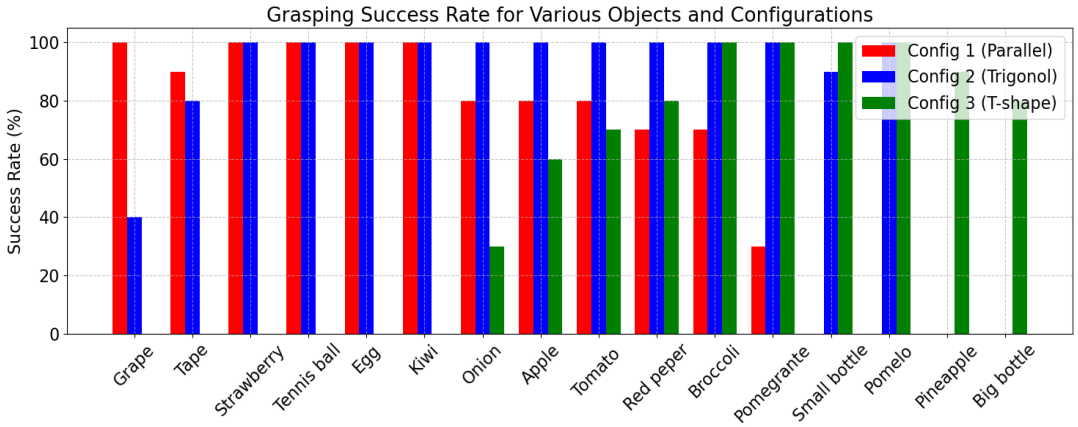

Fig. 6. Success rate of grasping various objects using different gripper configurations.

TABLE II. Testing Objects for grasping

Object	Weight	Dimensions (d × h)	Property
Grape	8 g	20 mm × 26 mm	Soft, smooth
Tape	20 g	54 mm × 16 mm	Rigid, smooth
Strawberry	20 g	34 mm × 43 mm	Soft, rough
Tennis Ball	55 g	65 mm × 65 mm	Soft, rough
Egg	60 g	43 mm × 53 mm	Rigid, smooth
Kiwi	117 g	57 mm × 70 mm	Soft, rough
Onion	144 g	67 mm × 64 mm	Rigid, rough
Apple	160 g	72 mm × 67 mm	Rigid, rough
Tomato	172 g	72 mm × 64 mm	Soft, smooth
Red Pepper	200 g	86 mm × 76 mm	Soft, rough
Broccoli	375 g	110 mm × 150 mm	Rigid, rough
Pomegranate	487 g	96 mm × 86 mm	Rigid, smooth
Small Bottle	515 g	60 mm × 200 mm	Soft, smooth
Pomelo	913 g	160 mm × 150 mm	Rigid, smooth
Pineapple	1210 g	110 mm × 210 mm	Rigid, rough
Big Bottle	1540 g	80 mm × 315 mm	Soft, smooth

Configuration 1 excels in the manipulation of smaller objects. Configuration 2 demonstrates the best overall performance and has a high success rate in terms of grasping medium-sized objects. In contrast, Configuration 3 particularly excels in grasping larger, elongated, heavier objects. In conclusion, the gripper's morphological differences enabled by reconfigurable design significantly enhance its grasping capabilities. The gripper has been tested and is capable of grasping objects ranging from 4 mm to 80 mm in radius. It is particularly effective at handling objects with spherical or cylindrical shapes, making it highly suitable for picking up fruits and vegetables when the gripper configuration is adjusted appropriately. This adaptability is crucial in real-world scenarios where a diversity of objects demands varied manipulation strategies.

B. Performance Evaluation for Different Algorithms

By equipping the gripper with a tactile sensor, two grasping stability detection methods are used to ensure a secure grasp on objects while applying minimal force. The experiment involves using the TacFR-Gripper to grasp objects. The gripping force is progressively increased until the tactile sensor indicates a transition from a 'Non-Graspable' status to a 'Graspable' condition. Subsequently, the gripper, mounted on a robotic arm, is lifted and subjected to vibration to test if it can maintain a secure grip on the objects. The evaluation is based on three key metrics:

- Success Rate: This metric evaluates how effectively the grasping stability detection prevents an object from falling during the grasp. A higher success rate indicates better stability.
- Time Cost: This metric measures the speed at which the gripper stabilized the successful grasping. Quick detection and response are crucial for efficient and timely robotic operations.
- Contact Force: This metric examines the amount of force applied during grasping to maintain a secure grip without applying excessive force, especially when manipulating delicate and soft objects. It is the most important metric in this experiment.

TABLE III. Comparative analysis between the threshold-based method, the GNN-based method, and manual control for object grasping.

	Threshold	GNN	Manual
Time (s)	6.5	2	4
Contact Force (N)	3.2	2.35	6.73
Success Rate (%)	80	80	100

Table.III shows that without the support of a tactile sensor, the contact force acting on the objects would significantly increase. Although the grasping success rate for manual operation is 100 %, such excessive contact force is unacceptable, resulting in potential damage to gripped objects, especially those with soft properties, such as fruits. This increase in force arises because the visual information alone is insufficient to accurately gauge how much force is necessary to maintain a secure grip. In this case, it is vital to utilize tactile information in object grasping.

In Table.III, the GNN method is triple more time-efficient than the threshold method. This improvement is primarily attributed to that GNN performs a more flexible classification of states as 'Graspable' rather than relying on a fixed threshold value, thereby enhancing both performance and reliability. The contact force applied by the GNN method is two-thirds of the threshold method's value. Remarkably, this reduction in force does not compromise the GNN

method's success rate in object pick-up. Such decreased force requirement demonstrates operational efficiency and several advantages, including a lower risk of damaging objects and enhanced energy efficiency.

During the grasping, the threshold method is limited by the fixed force threshold, each finger of the gripper would continuously adjust to bring all fingers within the threshold force range, often ignoring the fact that the object is already securely grasped, even if its position or orientation differs slightly from what was initially expected. This constant adjustment can lead to inefficiencies, notably longer periods of adjustment (oscillation period in Fig.4). Also, such a long adjustment time can be reduced by broadening the range of force we set for the threshold method. However, the enlarged range would also increase the force applied to the objects, asking for trade-off through a lot of fine-tuning.

In contrast, the GNN method, excels at learning complex and nonlinear relationships from non-Euclidean data [28], and incorporates a more comprehensive range of object states during its training phase. So it can accommodate a wider range of conditions, requiring no extra time on finger adjustments as the threshold method does. As a result, it can maintain optimal contact with the object throughout the manipulation process, regardless of changes in the grasping pose. This adaptability helps to save the extra effort required to adjust to each new object.

C. Evaluation of In-Hand Manipulation

In this experiment, we conducted a comparative analysis between dexterity workspace simulation outcomes and experimental data by letting the gripper manipulate daily life objects. As Fig. 7 indicated, by measuring the displacement at the center points, we were able to determine the maximum actual displacement occurring during the in-hand manipulation process. Our observations revealed a general alignment between most simulation results and the actual measurements. However, for heavier objects, specifically those heavier than 200 grams, the simulation efficacy was degraded. This discrepancy can be attributed to the deformation of the Fin Ray-based fingers upon contact with objects. Greater deformation results in an increased contact force. To maintain effective contact with heavier objects, the Fin Ray-based fingers must undergo more deformation, leading to a corresponding reduction in the displacement generated by the soft fingers during manipulation. Conversely, for lighter objects, the measured displacements were very close to those predicted by the simulation, proving its effectiveness. In the future, factors such as the object's shape, weight, and surface material will be incorporated into simulations.

To demonstrate the effective in-hand manipulation capability of the TacRF-Gripper, we assembled the gripper on a robotic arm and conducted a bottle cap removal task. The whole task can be segmented into four procedures (see Fig.8, P1-P4):

- Adjust Gripper Pose and Grasp (P1): This step involves determining the optimal angle for the robotic gripper's interaction with the bottle cap.

TABLE IV. Comparison between Maximum movement for manipulating different objects in the real world and simulation.

Radius	Weight	Simulation Movement	Real Movement
33 mm	55 g	16 mm	16 mm
33 mm	144 g	16 mm	19 mm
34 mm	172 g	20 mm	22 mm
35 mm	117 g	23 mm	27 mm
38 mm	260 g	28 mm	22 mm

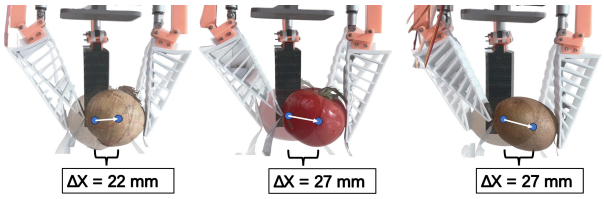

Fig. 7. Comparisons between the range of in-hand manipulation between the simulation from the workspace analysis and the physical experimental results for manipulating objects with various sizes and shapes. ΔX indicates the maximum in-hand object translation distance.

- Bottle Cap Rotation (P2): The robotic gripper rotates the bottle cap using a servomotor located at the base of its fingers while maintaining consistent contact.
- Reorientation and Iteration (P3): This procedure involves repositioning the pose of the robotic gripper and then repeating Procedures P1 and P2 iteratively until the cap becomes loose.
- Bottle Cap Lift-off (P4): In this final step, the robotic gripper grasps the cap with all three fingers and performs a lift-off action using the robot arm.

To assess the performance of bottle cap removal, experiments are conducted five times, with data collected specifically during 'Cap Rotation'. Whenever a 'Non-Graspable' status is detected, the servomotor stops to allow for re-grasping. Therefore, the iteration metric serves as an indicator of both the algorithm's efficiency and robustness in handling the task.

We compare the GNN-based and threshold-based approaches for this application. The results are summarized in Table.V. The GNN-based approach leads to reduced task durations, reduced contact force, and increased success rate compared to the threshold-based method.

TABLE V. Comparisons between the threshold-based and GNN-based approaches for the bottle cap removal task.

	Threshold Approach	GNN Approach
Time (s)	80.56	52.26
Contact Force (N)	5.5	4.3
Success rate (%)	72	88

V. Discussion and Conclusion

In this paper, we introduce the TacFR-Gripper, a reconfigurable Fin Ray-based soft tactile gripper capable of grasping and manipulating objects of various sizes. We incorporated a tactile sensor array onto the soft Fin-Ray finger, which can be known as the tactile skin. We utilize a GNN-based algorithm for tactile data processing, which significantly

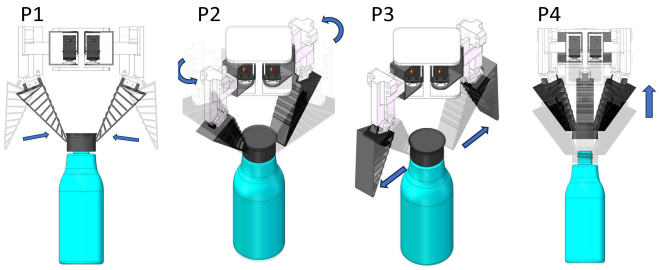

Fig. 8. Illustration of the procedures (P1-P4) for the bottle cap removal task.

enhances grasping detection capabilities. Through rigorous testing and comprehensive analysis, we demonstrate the TacFR-Gripper's proficiency in handling a wide range of delicate objects, and showing its potential applicability in a range of fields. Moreover, experimental comparisons indicate that the proposed GNN-based tactile perception approach outperforms threshold-based control methods in terms of accuracy and efficiency.

In our future work, we plan to integrate tactile skin across the entire gripper surface. More complex tasks will be carried out to further evaluate the capabilities of the TacFR-Gripper for contact-rich dexterous manipulation.

REFERENCES

[1] S. Alves, M. Babcinschi, A. Silva, D. Neto, D. Fonseca, and P. Neto, "Integrated design fabrication and control of a bioinspired multimaterial soft robotic hand," *Cyborg and Bionic Systems*, vol. 4, p. 0051, 2023.

[2] E. Almanzor, T. G. Thuruthel, and F. Iida, "Automated fruit quality testing using an electrical impedance tomography-enabled soft robotic gripper," in *2022 IEEE/RSJ International Conference on Intelligent Robots and Systems (IROS)*, 2022, pp. 8500–8506.

[3] H. DONG, M. BOZKURTTAS, R. MITTAL, P. MADDEN, and G. V. LAUDER, "Computational modelling and analysis of the hydrodynamics of a highly deformable fish pectoral fin," *Journal of Fluid Mechanics*, vol. 645, p. 345–373, 2010.

[4] M. H. Ali, A. Zhanabayev, S. Khamzhin, and K. Mussin, "Biologically inspired gripper based on the fin ray effect," in *2019 5th International Conference on Control, Automation and Robotics (ICCAR)*, April 2019, pp. 865–869.

[5] J. Shintake, V. Cacucciolo, D. Floreano, and H. Shea, "Soft robotic grippers," *Advanced Materials*, vol. 30, no. 29, p. 1707035, 2018.

[6] S. Q. Liu and E. H. Adelson, "Gelsight fin ray: Incorporating tactile sensing into a soft compliant robotic gripper," in *2022 IEEE 5th International Conference on Soft Robotics (RoboSoft)*, 2022, pp. 925–931.

[7] I. M. Bullock and A. M. Dollar, "Classifying human manipulation behavior," in *2011 IEEE International Conference on Rehabilitation Robotics*. Zurich: IEEE, Jun. 2011, pp. 1–6.

[8] W. Crooks, G. Vukasin, M. O'Sullivan, W. Messner, and C. Rogers, "Fin ray® effect inspired soft robotic gripper: From the robosoft grand challenge toward optimization," *Frontiers in Robotics and AI*, vol. 3, p. 70, 2016.

[9] Q. Lu, N. Baron, A. B. Clark, and N. Rojas, "Systematic object-invariant in-hand manipulation via reconfigurable underactuation: Introducing the RUTH gripper," *The International Journal of Robotics Research*, vol. 40, no. 12-14, pp. 1402–1418, Dec. 2021.

[10] Y. Cai and S. Yuan, "In-hand manipulation in power grasp: Design of an adaptive robot hand with active surfaces," in *2023 IEEE International Conference on Robotics and Automation (ICRA)*. IEEE, 2023, pp. 10 296–10 302.

[11] T. Sakuma, F. Von Drigalski, M. Ding, J. Takamatsu, and T. Ogasawara, "A universal gripper using optical sensing to acquire tactile information and membrane deformation," in *2018 IEEE/RSJ International Conference on Intelligent Robots and Systems (IROS)*. IEEE, 2018, pp. 1–9.

[12] S. Li, X. Yin, C. Xia, L. Ye, X. Wang, and B. Liang, "Tata: A universal jamming gripper with high-quality tactile perception and its application to underwater manipulation," in *2022 International Conference on Robotics and Automation (ICRA)*, 2022, pp. 6151–6157.

[13] J. Zhao and E. H. Adelson, "Gelsight svelte: A human finger-shaped single-camera tactile robot finger with large sensing coverage and proprioceptive sensing," *arXiv preprint arXiv:2309.10885*, 2023.

[14] W. Yuan, S. Dong, and E. H. Adelson, "Gelsight: High-resolution robot tactile sensors for estimating geometry and force," *Sensors*, vol. 17, no. 12, p. 2762, 2017.

[15] W. Fan, H. Li, W. Si, S. Luo, N. Lepora, and D. Zhang, "Vitactip: Design and verification of a novel biomimetic physical vision-tactile fusion sensor," *arXiv preprint arXiv:2402.00199*, 2024.

[16] J. H. Low, P. M. Khin, Q. Q. Han, H. Yao, Y. S. Teoh, Y. Zeng, S. Li, J. Liu, Z. Liu, P. V. y Alvarado *et al.*, "Sensorized reconfigurable soft robotic gripper system for automated food handling," *IEEE/ASME Transactions On Mechatronics*, vol. 27, no. 5, pp. 3232–3243, 2021.

[17] K. Batsuren and D. Yun, "Soft robotic gripper with chambered fingers for performing in-hand manipulation," *Applied Sciences*, vol. 9, no. 15, p. 2967, Jul. 2019.

[18] A. Pagoli, F. Chapelle, J. A. Corrales, Y. Mezouar, and Y. Lapusta, "A soft robotic gripper with an active palm and reconfigurable fingers for fully dexterous in-hand manipulation," *IEEE Robotics and Automation Letters*, vol. 6, no. 4, pp. 7706–7713, 2021.

[19] S. Jain, T. Stalin, V. Subramaniam, J. Agarwal, and P. V. y Alvarado, "A soft gripper with retractable nails for advanced grasping and manipulation," in *2020 IEEE International Conference on Robotics and Automation (ICRA)*, 2020, pp. 6928–6934.

[20] D. Zhang, J. Liu, A. Gao, and G.-Z. Yang, "An ergonomic shared workspace analysis framework for the optimal placement of a compact master control console," *IEEE Robotics and Automation Letters*, vol. 5, no. 2, pp. 2995–3002, 2020.

[21] J. S. Dai, D. Wang, and L. Cui, "Orientation and workspace analysis of the multifingered metamorphic hand—metahand," *IEEE Transactions on Robotics*, vol. 25, no. 4, pp. 942–947, 2009.

[22] D. Zhang, J. Liu, L. Zhang, and G.-Z. Yang, "Design and verification of a portable master manipulator based on an effective workspace analysis framework," in *2019 IEEE/RSJ International Conference on Intelligent Robots and Systems (IROS)*. IEEE, 2019, pp. 417–424.

[23] J. Li, F. Zhao, X. Li, and J. Li, "Analysis of robotic workspace based on monte carlo method and the posture matrix," in *2016 IEEE International Conference on Control and Robotics Engineering (ICCRE)*, 2016, pp. 1–5.

[24] D. Zhang, F. Cursi, and G.-Z. Yang, "Wsrender: A workspace analysis and visualization toolbox for robotic manipulator design and verification," *IEEE Robotics and Automation Letters*, vol. 4, no. 4, pp. 3836–3843, 2019.

[25] SciPy Development Team, "scipy.stats.gaussian_kde — SciPy v1.11.3 Manual," 2023.

[26] T. N. Kipf and M. Welling, "Semi-supervised classification with graph convolutional networks," *arXiv preprint arXiv:1609.02907*, 2016.

[27] H. Zhu and P. Koniusz, "Simple spectral graph convolution," in *International conference on learning representations*, 2020.

[28] W. Fan, H. Bo, Y. Lin, Y. Xing, W. Liu, N. Lepora, and D. Zhang, "Graph neural networks for interpretable tactile sensing," in *2022 27th International Conference on Automation and Computing (ICAC)*, 2022, pp. 1–6.